



Environmental
Science
Nano

Emerging investigator series: Linking Chemical Transformations of Silver and Silver Nanoparticles in the Extracellular and Intracellular Environment to their Bio-reactivity.

Journal:	<i>Environmental Science: Nano</i>
Manuscript ID	EN-COM-06-2019-000710.R1
Article Type:	Paper
Date Submitted by the Author:	09-Aug-2019
Complete List of Authors:	Minghetti, Matteo; Oklahoma State University Stillwater, Dudefoi, William; Oklahoma State University Stillwater Ma, Qing; Northwestern Synchrotron Research Center at the Advanced Photon Source, Catalano, Jeffrey; Washington University, Earth & Planetary Sciences

SCHOLARONE™
Manuscripts

1
2
3 **Emerging investigator series: Linking Chemical Transformations of Silver and Silver**
4 **Nanoparticles in the Extracellular and Intracellular Environment to their Bio-reactivity.**
5
6
7

8
9 Matteo Minghetti,^a William Dufey,^a Qing Ma,^b and Jeffrey G. Catalano^c
10
11

12
13 a. Department of Integrative Biology, Oklahoma State University, Stillwater, OK, USA.
14

15 b. DND-CAT, Northwestern Synchrotron Research Center at Advanced Photon Source,
16 Argonne, IL, USA.
17

18 c. Department of Earth and Planetary Sciences, Washington University, Saint Louis, MO, USA.
19
20
21
22
23
24
25
26
27
28
29

30 # Corresponding author
31

32
33 Address: Department of Integrative Biology, 501 Life Sciences West, Oklahoma State University,
34 Stillwater, OK 74078.
35

36
37
38 Email: matteo.minghetti@okstate.edu
39
40
41
42
43
44
45
46
47
48
49
50
51
52
53
54
55
56
57
58
59
60

Abstract

The fish intestine is an important barrier for environmental toxicants, including metals and metal nanoparticles. Tracking chemical transformation at the interface between the intestinal epithelium and the intestinal lumen can inform us about chemicals' bio-reactivity and toxicity but is challenging due to the lack of appropriate models. To allow for such investigations, a model of the fish intestine derived from rainbow trout (*Oncorhynchus mykiss*), the RTgutGC cell line, was used. Cells were exposed to silver nitrate (AgNO_3) or citrated coated silver nanoparticles (cit-AgNP) in Leibovitz's L-15 medium without amino acids and vitamins (L-15/ex), which allowed the determination of the extracellular silver species using a chemical equilibrium model. X-ray absorption spectroscopy (XAS) was used to track the intracellular silver speciation. Cellular toxicity, silver accumulation, and metallothionein (MT) mRNA levels were also measured. Cells accumulated the same concentrations of silver when exposed to equimolar amounts (i.e. 1, 5 and 10 μM) of AgNO_3 or cit-AgNP. However, AgNO_3 was shown to be more toxic than cit-AgNP. Intracellular silver speciation changed over time in both exposure series. After 1-hour, intracellular silver speciation was dominated by chloride complexation in both exposures. After 24 and 72 hours of exposure to cit-AgNP, ~ 7% of silver were complexed to cysteine whereas the remaining silver was AgNP. In cells exposed to AgNO_3 for 72 hours, 97% Ag was complexed to cysteine. A significant increase, compared to controls, in metallothionein mRNA levels at 24 and 72 hours of exposure to AgNO_3 and cit-AgNP can explain the formation of Ag-cysteine complexes. In sum, these data show that silver chloride species are bioavailable and that complexation to cysteine scavenges intracellular dissolved silver ions thus preventing toxicity. Silver nanoparticles present a similar but attenuated toxic response to AgNO_3 . Thus, at least in acute exposures, existing risk assessment for dissolved silver species could be protective for nanosilver.

Keywords: silver nanoparticles, X-ray absorption spectroscopy, RTgutGC, silver speciation

Environmental Significance Statement

The antimicrobial properties of silver nanoparticles are being exploited in numerous applications, including food supplements and disease control in aquaculture, which may result in their dietary uptake by aquatic organisms. Our knowledge of the precise mechanism of uptake of silver and nano silver via the dietary route at the intestine is limited due to lack of an appropriate model to study interactions at the cell/medium interface. For instance, the bioavailability and toxicity of chloride complexes, which might form readily after silver nanoparticles intestinal dissolution, is poorly understood. By determining the relationship between extracellular and intracellular metal speciation, we can evaluate the bioavailability and toxicity of specific metal species. This information may prove instrumental in implementing new models for nanoparticles environmental risk assessment.

1. Introduction

Silver nanoparticles (AgNP) are clusters of silver atoms ranging from 1 to 100 nm in all three external dimensions¹ which, due to their increased antimicrobial properties, are used in a plethora of applications such as food additives, food packaging materials and water disinfectants². Silver nanoparticles have also been proposed as effective alternatives to antibiotics for human and veterinary medicine^{3,4}, and, more recently, the use for disease control in aquaculture has been suggested⁵. The use of AgNP in these applications may result in the absorption of this material via the intestinal route both in humans and fish as environmental species. Despite the advantages that this technology brings about, their impact on human and environmental health is of concern² especially considering that absorptive processes at the intestine are currently poorly understood.

1
2
3 In order to understand the physiological role and toxicology of metals in dissolved or in
4 colloidal form in the natural environment, one needs to be aware of the speciation of metals in
5 abiotic and biotic compartments. The chemical species in which a metal is present in the
6 extracellular environment (i.e., at the interface with the absorptive epithelium) determines its
7 binding potential to biological ligands including glycoproteins present in the mucus and
8 membrane proteins, which might reduce or enhance the uptake into the cell. Several studies
9 have shown that the environmental (i.e., in the water column) free metal ion concentration can
10 be a better predictor of metal toxicity in aquatic organisms than the total dissolved
11 concentration⁶. However, metal speciation can vary significantly while transitioning from the
12 water column to the extracellular environment. For instance, in fresh water, chloride
13 concentration might be low (~0.03 to ~5 mM) while at the absorptive epithelium of the fish
14 intestine it might be much higher (~70 to 150 mM)⁷ resulting in the formation of different metal
15 species⁸. There is also emerging evidence that metal complexes can present enhanced
16 bioavailability⁹ and that neutral¹⁰, negatively, and positively charged metal complexes can be
17 bioavailable and toxic^{8,9,11,12}; further studies of these mechanisms might have useful implications
18 for environmental risk assessment.

19
20
21
22
23
24
25
26
27
28
29
30
31
32
33
34
35
36
37 While the non-essential metal silver enters the cells by leaching through essential metal
38 transposers^{13,14}, AgNP seem to bypass such mechanisms and enter the cell via
39 endocytosis^{11,15,16}. Therefore, MeNP uptake might be more difficult to control by the cell,
40 resulting in the entry of a 'big' cargo of zero-valent MeNP into cellular vesicles. Depending on
41 the vesicle's internal milieu and MeNP solubility, metal ions will dissolve and possibly be
42 transported out into the cytoplasm via metal transporters¹⁷ leaving the nano-material behind.
43 The dissolved metal ion will then form different chemical species that will determine metal
44 reactivity with cellular components, thus metal bio-reactivity and toxicity. For instance, certain
45 NPs, such as AgNP, seem to be directed to lysosomes whose internal milieu is characterized by
46
47
48
49
50
51
52
53
54
55
56
57
58
59
60

1
2
3 an acidic pH that likely induces dissolution of silver from the NP surface¹¹. In addition, while
4 commercial products might contain pristine AgNP, in natural water chemical transformations
5 such as sulfidation have been shown to have an important role in determining toxicity of silver
6 nanoparticles (AgNP) to aquatic organisms¹⁸. The decrease in AgNP toxicity appears to be
7 related to the complexation with HS⁻. Moreover, while fish exposure to pristine AgNP could be
8 relevant in aquaculture, where pristine AgNP use has been proposed to improve water quality
9 and for disease control⁵, AgNP may also readily associate with environmental ligands (e.g.,
10 nutrients and other natural colloids). Therefore, determination of chemical transformations of
11 metal NPs in the exposure medium (i.e., complexation of the metal ions dissolving from the NPs
12 surface) is necessary to understand their bioavailability and toxicity. While these considerations
13 have been shown to be extremely useful in predicting toxicity of waterborne AgNP to fish
14 embryos^{19,20}, they might not apply to dietary exposures. Indeed, we know very little about the
15 chemical transformations that might occur in the intestinal lumen of fish - partially due to the lack
16 of appropriate models to study such phenomena. Indeed, a better understanding of chemical
17 transformations in the intracellular environment is necessary to predict nanoparticle bio-
18 reactivity and toxicity.

19
20
21
22
23
24
25
26
27
28
29
30
31
32
33
34
35
36
37 To allow for such investigations at the NP/cell interface, we used a model of the fish
38 intestine derived from Rainbow Trout (*Oncorhynchus mykiss*), the RTgutGC cell line²¹.
39 RTgutGC is a unique intestinal fish cell line, which, when grown on permeable supports
40 (transwells), forms a cell monolayer dividing the system into an upper (apical) and a lower
41 (basolateral) compartment, thereby mimicking the intestinal lumen and the portal blood,
42 respectively (Figure 1). RTgutGC cells grown on transwells develop a polarized epithelium
43 characterized by expression of tight junction (ZO-1) and Na/K-ATPase proteins at the apical and
44 basolateral membrane respectively²¹. Most importantly, RTgutGC cells tolerate exposures to
45 well-defined synthetic simplified media that mimic different possible environmental scenarios
46 (e.g. pH, salinity, presence of proteins, etc.) occurring at the intestinal lumen, thus allowing the
47
48
49
50
51
52
53
54
55
56
57
58
59
60

1
2
3 study of NP interactions with the media components and, once internalized, with the intracellular
4 environment. In a recently study, it was shown that AgNP bioavailability and toxicity in the
5 intestine is linked to the composition of its luminal content¹¹. Although the RTgutGC cell culture
6 system represents a less complex model in comparison to the intact fish intestine, it offers
7 advantages in comparison to in vivo models such as easier manipulations of the luminal
8 medium. Also, in comparison to ex vivo models (i.e., gut sac) it offers an easier high-throughput
9 approach and allows longer exposure times²¹. The RTgutGC cell system is also more ethical
10 reducing the burden on animal testing.
11
12

13
14 The agglomeration and dissolution of MeNPs and the speciation of the resulting aqueous
15 metals in the exposure media can be determined in simplified media of known composition^{11,22}
16 (Figure 1). Speciation of metal in a simplified exposure medium can be achieved by using
17 chemical equilibrium models. However, determination of intracellular MeNPs' transformations
18 and the speciation of the metal ions released from the NP surface is challenging. It was shown
19 recently that by feeding relevant stability constants into chemical equilibrium models allows the
20 simulation of intracellular chelation reactions²³. However, chemical equilibrium models are not
21 comprehensively parameterized for the complex intracellular environment and are not designed
22 to predict the transformations that metal nanoparticles can undergo in such environment.
23
24 Electron microscopy and Raman spectroscopy techniques are sensitive to MeNPs but cannot
25 detect dissolved or biomolecule-bound metals. In contrast, X-ray absorption spectroscopy (XAS)
26 is optimally suited for the non-destructive determination of the speciation of metals *in situ*, even
27 at low concentrations, or when metal occurs as diffuse dissolved or complexed species rather
28 than concentrated particles²⁴. Therefore, the use of chemical equilibrium models in conjunction
29 with *in situ* XAS measurements allows to study the link between extracellular metal speciation
30 with intracellular metal speciation. In this study, RTgutGC cells were cultured on transwells
31 allowing the formation of a polarized epithelium²¹ to simultaneously track intracellular silver
32
33
34
35
36
37
38
39
40
41
42
43
44
45
46
47
48
49
50
51
52
53
54
55
56
57
58
59
60

1
2
3 accumulation, speciation and bioreactivity following exposure to silver nitrate and silver
4 nanoparticles.
5
6
7

8 9 **2. Experimental**

10 **2.1 RTgutGC cell culture**

11
12 RTgutGC were kindly gifted by Kristin Schirmer (Eawag, CH). Preparation of the polarized
13 RTgutGC epithelium was performed exactly as described previously²¹. Briefly, RTgutGC cells
14 were seeded at 62,500 cells/cm², counting cells with the Countess II™ Automated Cell Counter
15 (Thermofisher, Waltham, MA, USA) onto transparent tissue culture inserts for multiwell plates
16 (pore size = 0.4 µm; polyethylene terephthalate [PET] from Greiner Bio-One, Monroe, NC,
17 USA). Insert size was chosen depending on the application (see the following): 0.33 cm² inserts
18 (for 24-well plates) for cell viability, and 4.52 cm² inserts (for 6-well plates) for quantitative PCR
19 (qPCR), silver quantification by ICP-MS and XAS analysis. RTgutGC cell were culture in
20 symmetrical conditions (i.e., with identical medium in the apical and basolateral chamber) in in
21 Leibovitz's L-15 medium without phenol red (Thermofisher, Waltham, MA, USA) supplemented
22 with 5% foetal bovine serum (FBS, Cat. No. F2442, Sigma-Aldrich, St. Louis, MO, USA) and 1%
23 gentamicin (10 mg/mL, Gibco, Thermofisher, Waltham, MA, USA). The medium was changed
24 weekly and trans epithelial electrical resistance (TEER) was monitored before medium change
25 using an epithelial tissue voltohmeter (EVOM2; World Precision Instruments, USA) fitted with
26 chopstick electrodes (STX-2). In all cases TEER reached 30 ohms* cm² by 21 days. All
27 experiments were performed on RTgutGC cells cultured on inserts for 21 days.
28
29
30
31
32
33
34
35
36
37
38
39
40
41
42
43
44
45
46
47
48
49

50 **2.2 Exposures**

51 All exposures were performed as previously described¹¹. Citrate coated silver NP were
52 purchased as aqueous suspension with a concentration of total silver of 1 g/L (9.27mM, pH =
53 6.46). Experimental solutions were prepared freshly in the exposure medium L-15/ex¹¹. L-15/ex
54
55
56
57
58
59
60

1
2
3 has identical salts and sugars composition to the commercial cell culture media Leibovitz's L-15
4 (Gibco/ Thermofisher, Waltham, MA, USA) but does not contain amino acids and vitamins.
5
6 Every batch of L-15/ex was measured and kept at pH of 7.2. All exposures were performed in
7
8 normal atmosphere incubated at 19 °C. All exposures were performed in normal atmosphere
9
10 incubated at 19 °C. Silver nitrate (Sigma-Aldrich, St. Louis, MO, USA) stock solution was
11
12 prepared at a concentration of 10 mM in nanopure water (16–18 MΩcm⁻¹ Barnstead GenPure
13
14 Water, Thermofisher, Waltham, MA, USA) and diluted right before each experiment in L-15/ex.
15
16 Silver nitrate and cit-AgNP stock solutions were prepared to contain identical nominal
17
18 concentrations of total silver. The citrate coated silver nanoparticles (cit-AgNP, nominal size: 19
19
20 nm, NanoSys GmbH, Wolfhalden, Switzerland) characterization in the exposure medium L-
21
22 15/ex is reported in Figure 2. The nanoparticle agglomerate (Z-average) size and zeta potential
23
24 of cit-AgNP were measured by dynamic light scattering (DLS) and electrophoretic mobility using
25
26 a Zetasizer (Nano ZS, Malvern Instruments, Malvern, UK). Citrate coated AgNP dissolution was
27
28 measured by ultracentrifugation as previously described²². Twenty-five mL of cit-AgNP
29
30 suspensions were centrifuged at 145000 g (Beckman Coulter, Optima XE-90 Ultracentrifuge) for
31
32 3 h. A volume of 1 mL supernatant was digested with 0.725 mL of 69% HNO₃ for 1 hour at room
33
34 temperature. The digests were diluted 10-times and measured by inductively coupled plasma-
35
36 mass spectrometer (ICP-MS, iCAP Qc Thermo Scientific, USA). The recovery of AgNO₃ in ultra-
37
38 centrifugation was over 98%. The reliability of the measurements was determined using specific
39
40 water references (CPI International, USA). After 21 days of culture on transwells²¹, the polarized
41
42 epithelium was washed twice with a phosphate buffer (PBS, Gibco, Thermofisher, Waltham,
43
44 MA, USA) then cit-AgNP or AgNO₃ suspensions were applied at concentrations ranging from
45
46 0.1 to 54 μg/mL in L-15/ex to determine the dose-response curve. In addition, to compare the
47
48 toxicity and accumulation of AgNO₃ and cit-AgNP cells were exposed in parallel experiments to
49
50 the same concentrations of AgNO₃ and cit-AgNP (i.e., 5 and 10 μM total Ag) and then viability
51
52
53
54
55
56
57
58
59
60

1
2
3 and silver uptake were measured. Furthermore, three identical sets of polarized RTgutGC were
4 exposed to non-toxic doses of AgNO₃ (1 μM) and cit-AgNP (10 μM or 1.08 μg/mL) for 1, 24 and
5 72 hours: i) intracellular metal concentration by ICP-MS ii) messenger RNA quantification by
6 quantitative RT-PCR and iii) intracellular metal speciation by XAS.
7
8
9
10

11 12 13 **2.3 Assessment of cell viability**

14 Following exposure, the polarized RTgutGC cells have been washed twice with PBS.

15
16 Assessment of cell viability was performed by means of the fluorescent dyes, Alamar blue (AB;
17 ThermoFisher, Waltham, MA, USA), 5-carboxyfluorescein diacetate acetoxyethyl ester (CFDA-
18 AM; ThermoFisher, Waltham, MA, USA) and Neutral Red (NR; Sigma-Aldrich, St. Louis, MO,
19 USA) which are indicators of cell metabolic activity, cell membrane integrity and lysosome
20 integrity as previously described²⁵. Fluorescence was recorded using a Cytation5 plate reader
21 (BioTek, USA) at respective excitation/emission wavelengths of 530/595 nm for AB, 485/530 nm
22 for CFDA-AM and 530/635nm for NR.
23
24
25
26
27
28
29
30
31
32
33

34 **2.4 Quantification of intracellular silver accumulation**

35
36 Intracellular silver concentration was measured by ICP-MS. Following exposure, silver
37 determination in the polarized RTgutGC cells has been performed as previously described²⁵. To
38 ensure thorough removal of loosely bound silver, the cells were washed twice with a solution of
39 0.5 mM cysteine in PBS. The cells were then lysed by applying 1 mL of 50 mM NaOH to the
40 well and incubated at room temperature for 2 hours. An aliquot (100 μL) of the cells' lysate was
41 used for protein quantification using the modified Lowry assay (Thermo Scientific, Waltham,
42 USA). For metal determination, cell lysates were desiccated using a concentrator (Concentrator
43 Plus, Eppendorf, Hamburg, Germany) and digested overnight by adding 0.8 mL of 69% HNO₃.
44 Acidified solutions were then resuspended and transferred to a Teflon tube containing 0.2 mL of
45 30% H₂O₂ and digested further in a digestion system (PicoTrace GmbH, Bovenden, Germany)
46
47
48
49
50
51
52
53
54
55
56
57
58
59
60

1
2
3 at a maximum temperature of 180°C for 30 minutes. The digest was then diluted 10 times with
4 nanopure water and measured. The reliability of the measurement was determined using
5 specific references (CPI International, USA). Silver concentration in cell lysates is reported as
6 ng Ag per mg of protein determined from the same samples to take into account cell growth.
7
8
9

10 11 12 13 **2.5 Quantification of Metallothionein mRNA levels**

14
15
16 Metallothionein mRNA levels in RTgutGC were measured exactly as previously described¹¹.
17
18
19

20 21 **2.6 Determination of intracellular silver species by X-ray absorption spectroscopy:**

22 After exposure cells were washed twice times with Versene solution (0.48 mM EDTA in PBS,
23 Thermo Fisher Scientific, USA) and dislodged by trypsinization (0.25% Trypsin/EDTA solution in
24 PBS, Gibco, Thermofisher, Waltham, MA, USA). The trypsinization reaction was stopped by re-
25 suspending the cells in L-15 medium supplemented with 5% FBS. Afterword cells were washed
26 by centrifugation at 500 g for 3 minutes and re-suspension in L-15/ex. Cell viability in the
27 washed cells was checked using the trypan blue exclusion assay with the automated cell
28 counter Countess II (Thermofisher, Waltham, MA, USA) and was always over 90%. Finally, cells
29 were pelleted by centrifugation at 500 g for 3 minutes the supernatant was aspirated and the
30 pellet was immediately frozen in liquid nitrogen and placed on a sample holder made of Kel-F®,
31 sealed with Kapton tape, and stored at -80°C. This prevented cell damage, shut down cell
32 activity, and inhibited oxidative or chemical alteration of silver during transport or data
33 collection²⁶. The samples were transported to the Advanced Photon Source (APS) frozen on dry
34 ice in sealed sample holders.
35
36
37
38
39
40
41
42
43
44
45
46
47
48
49

50 At the APS, these holders were mounted in a Linkham THMS6000 stage cooled to 77K with
51 liquid N₂ at beamline 5-BM-D. Fluorescence yield X-ray absorption near-edge structure
52 (XANES) spectra (Figure 5) were collected at the Ag K-edge using a pair of 4-element Vortex
53
54
55
56
57
58
59
60

1
2
3 energy dispersive Si-drift detectors. Eight to twelve spectra were collected for each sample and
4 then averaged to obtain the reported data. The incident beam energy was scanned using a
5 Si(111) double-crystal monochromator. The energy was calibrated using a Ag metal foil, with
6 the first inflection point in the Ag K-edge set to 25.514 keV. The spectra of known Ag
7 compounds (Figure S2) were collected in transmission or in total fluorescence yield using a
8 PIPS detector, with samples mounted as dry powders on cellulose acetate tape. A silver-
9 cysteine complex was prepared by modifying a procedure for Zn-cysteine complexes²⁷. 84.8 mg
10 of L-cysteine was added to 10 mL of 7 mM AgNO₃. The resulting acidic pH was neutralized to
11 pH 7 with 0.27 mL 1 M NaOH. The solution was then freeze dried and the powder was mounted
12 on tape. The spectrum of AgCl was taken from Sekine et al., (2015)²⁸.

13
14 While quantitative Ag contents were not determined, the relative concentration of Ag in each
15 sample was obtained from the change in Ag K_α X-ray fluorescence intensity across the K
16 absorption edge, i.e., the edge step²⁹. The spectra were background subtracted and normalized
17 in the Athena interface³⁰ to IFEFFIT³¹. Target transformation³² using three components well
18 reconstructed the spectra of AgCl, AgNP, Ag-cysteine, and Ag₂S. Ag-cysteine and Ag₂S have
19 similar XANES spectra (Figure S2), with subtle difference in fine structure at the edge and in the
20 position of oscillations above 25530 eV. Both spectra were reconstructed well except for the
21 broad feature centered near 25570 eV, which is more intense for Ag₂S and was not fully
22 reproduced. Given this analysis and the expression of cysteine-rich MT upon Ag exposure
23 (Figure 4), Ag-cysteine was used in subsequent fitting of the spectra, although the current data
24 cannot rule out the formation of Ag₂S. The spectra of AgNP and bulk metallic Ag are also
25 visually similar (Figure S2) but the bulk metal has larger amplitude oscillations above the
26 absorption edge, and this amplitude was not accurately reproduced via target transformation.
27 Silver speciation in the samples was then determined using linear-combination fitting of the
28 XANES spectra. Samples exposed to dissolved AgNO₃ were fitted using the spectra of AgCl
29 and Ag-cysteine. Fitting of the spectra of samples exposed to AgNPs included these two
30
31
32
33
34
35
36
37
38
39
40
41
42
43
44
45
46
47
48
49
50
51
52
53
54
55
56
57
58
59
60

1
2
3 spectral standards along with the spectrum of AgNP. All spectra were well reproduced (Figure
4
5 5) with component sums close to 1.
6
7

8 **2.6 Data analysis**

9
10 Statistical analysis was performed using GraphPad Prism Version 7.0 (GraphPad Software Inc.,
11 San Diego, CA). Fluorescent units obtained in the cell viability assays were converted to
12 percentage viability of control cells. The non-linear regression sigmoidal dose-response curve
13 fitting module using the Hill slope equation was used to fit the dose-response curve data.
14
15 Statistical analysis for multiple groups of data was performed by the analysis of variance
16 (ANOVA) followed by Tukey's post hoc test. When comparing to a control group, Dunnett's test
17 was applied after the ANOVA. Values of $p < 0.05$ were considered statistically significant.
18
19
20
21
22
23
24
25
26
27

28 **3 Results and Discussion**

29 **3.1 Citrate coated AgNP characterization in exposure medium**

30
31 Citrate coated AgNP at 10 μM show a size distribution of 84 ± 7 nm immediately after
32 preparing the solution in L-15/ex (i.e., time 0) and agglomerate rapidly reaching 795 ± 33 nm in
33 size with a z-potential of about -18 mV within 24 hours, after which agglomerate size remains
34 stable for at least 72 hours (Figure 2). Citrate coated AgNP dissolution in L-15/ex is about 6%
35 as determined by ultracentrifugation (Figure 2). The characterization of the same cit-AgNP in L-
36
37
38
39
40
41
42
43
44
45
46
47
48
49
50
51
52
53
54
55
56
57
58
59
60

59 **3.2 Cell viability studies**

60
Previous *in vitro* studies looking at the intracellular toxicity and chemical transformations of
AgNP focused on mammalian *in vitro* models where cells were exposed in complete medium
containing 5-10% FBS^{16,33-35}, therefore mimicking the exposure of cells to bloodborne silver. In
the blood AgNP or silver salts would reach the cells typically complexed to proteins and/or

1
2
3 amino acids. The uptake process and intracellular transformation of silver and silver
4 nanoparticle in absence of proteins or amino acids i.e., in polarized fish gut cells might be
5 different from that of non-polarized mammalian cells exposed in presence of FBS. Importantly,
6 aminoacidic complexation lowers toxicity most likely due to complexation of dissolved silver
7 from the AgNP surface by amino acids and proteins¹¹. For instance, it was previously shown
8 that the presence of amino acids ameliorates significantly silver nitrate and cit-AgNP toxicity due
9 to complexation of silver ions with cysteine^{11,36}. For cell types which are normally surrounded by
10 the blood, such an exposure scenario is relevant because it represents the route of exposure *in*
11 *vivo*. However, for studies using a polarized intestinal epithelium it is also relevant to study
12 exposures with and without amino acids and protein which is physiologically relevant^{25,37}. In this
13 study, silver nitrate and cit-AgNP were dissolved or dispersed in the exposure medium L-15/ex¹¹
14 which does not contain amino acids. In L-15/ex, dissolved silver is mostly present as negatively
15 charged silver chloride complex (AgCl_2^-) (Figure S1). The cell viability studies showed that silver
16 nitrate is more toxic than cit-AgNP after 24 hours of exposure in RTgutGC polarized cells
17 (Figure 3). Indeed, equimolar amounts of cell associated silver (Figure 3C) resulted in a different
18 toxicity response in RTgutGC (Figure 3B). Moreover, as shown previously^{11,22,25}, the multiple
19 endpoint assay indicated that lysosomes are the target of cit-AgNP whereas AgNO_3 affects
20 more cell metabolic activity (Figure 3B).

21
22 For the silver uptake, silver speciation and MT mRNA quantification cells were exposed to
23 non-toxic doses of silver nitrate and cit-AgNP (Figure 3A) for 1, 24 and 72 hours. In a previous
24 study, it was shown that cit-AgNP toxicity in RTgutGC reached a maximum at 24 hours and then
25 remained constant until 72 hours¹¹. Therefore, the highest non-toxic exposure concentrations (1
26 μM AgNO_3 or 10 μM equivalent of cit-AgNP; Figure 3A) were applied to polarized RTgutGC to
27 allow quantification of intracellular silver by ICP-MS and detection of intracellular silver species
28 by XAS but without compromising the overall cell health.

3.3 AgNO₃ and cit-AgNP uptake over time

Silver accumulated in RTgutGC cells in a linear and time dependent manner (Figure 4A). Moreover, RTgutGC cells exposed to 10 μM equivalent of cit-AgNP accumulated a maximum of 3.7-fold more silver in comparison to cells exposed to 1 μM AgNO₃, which suggests that the latter is more bioavailable. However, the accumulation of cit-AgNP was faster in cells as shown by the higher slope of the intracellular silver vs time linear relationship (figure 4A and SI). The faster accumulation could be explained by the nanoparticle agglomeration behavior in L-15/ex medium which might result in an incremental precipitation over time (Figure 2). Silver accumulation in RTgutGC could also be deduced by the fluorescence counts per seconds (Table S1). Although this quantification can only be considered as semi-quantitative the fluorescence counts gave a comparable silver accumulation over time, especially in cells exposed to cit-AgNP.

3.4 Intracellular silver speciation and MT mRNA abundance after exposure to AgNO₃ or cit-AgNP over time

Analysis of the X-ray absorption near-edge structure (XANES) region of XAS data (Figure 5) indicated that intracellular silver speciation changed over time in both exposure series (Figure 6). Principal component analysis on the six sample spectra required three components to reconstruct all data adequately, suggesting that three species are present in the sample set. At the earliest time point (1 hour) intracellular silver speciation is dominated by chloride complexation in both exposures. After one hour of exposure, cells exposed to AgNO₃ showed ~90% of Ag present as AgCl species and ~10% as Ag-cysteine complex. Cells exposed to cit-AgNP showed 78% of Ag present as AgCl and 18% as Ag⁰-NP. The presence of Ag complexed to cysteine is uncertain as the abundance of this species was within error of zero. Although the cells were washed twice with Versene (0.48 mM EDTA in PBS) to remove loosely bound metal,

1
2
3 we cannot exclude that some silver could be adsorbed on the cells and not necessarily be
4 internalized. Alternately the silver chloride complexes could enter the cells via: i) passive
5 diffusion if neutral complexes are formed¹⁰ or ii) AgCl could be reduced at the cell membrane,
6 silver could then enter as a free ion via copper transporters (e.g., CTR1^{14,38,39}) and then readily
7 re-complex with chloride, which is abundant in the cell cytoplasm. Intracellular silver chloride
8 complexation has previously been reported in neuronal cell lines after 24 hours of exposure to
9 AgNP (10-30% of total silver species¹⁶) and in a hepatic cell line exposed for 6 and 24 hours (2-
10 4% of total silver species⁴⁰). In our study, the percentage of detected silver chloride is higher.
11 This could be explained by the extracellular silver speciation (Figure S1). In L-15/ex silver
12 chloride is the dominant species whereas in the mammalian studies mentioned above,
13 exposures were performed in media containing amino acid and FBS, which would readily
14 complex with dissolved silver thus reducing the extracellular silver chloride concentration.
15 Moreover, these data suggest that, at early time points, i.e. after one hour of exposure, most
16 silver is adsorbed on the cell membrane or is internalized as dissolved silver chloride. Silver
17 chloride complexation dominates also in cells exposed to AgNO₃ for 24 hours and then shifts to
18 being complexed by cysteine, or possibly as Ag₂S (Figure S2), in cells exposed for 72 hours.
19 Although formation of Ag₂S inert precipitates have been previously shown in individual exposed
20 chronically to silver⁴¹, complexation with cysteine fit better our results due to the massive
21 induction of the cysteine rich protein, MT mRNA at 24 hours, and, to a smaller extent at 72
22 hours of exposure (Figure 4B). Obtaining XAS spectra into the extended X-ray absorption fine
23 structure (EXAFS) region, was not possible in the present study because of the noise level in
24 the data, and imaging via transmission electron microscopy coupled with energy-dispersive
25 spectrometry is needed to unambiguously distinguish the presence of silver cysteine complexes
26 from Ag₂S precipitates in RTgutGC.

27
28
29
30
31
32
33
34
35
36
37
38
39
40
41
42
43
44
45
46
47
48
49
50
51
52
53
54 The silver uptake data in combination with the XAS data suggests that cit-AgNP uptake is
55 gradual (Figure 4A, 6 and Table S1). Initially, i.e., after one hour of exposure, dissolved silver
56
57
58
59
60

1
2
3 chloride species were the most abundant species entering or adsorbing to the cell while cit-
4 AgNP uptake required more time. After 24 hours and 72 hours, cit-AgNP is internalized by
5 endocytosis and accumulates into the lysosomes as shown by the reduced lysosome
6 membrane integrity in the viability studies (Figure 3B and^{11,25}). After 24 and 72 hours of
7 exposure over >90% of intracellular silver is present as Ag⁰-NP and the remaining silver is
8 present as a complex with cysteine. Therefore, these data show that internalized cit-AgNP stay
9 mainly as reduced Ag⁰-NP for up to 72 hours in RTgutGC cells. About 5-7% of silver might
10 dissolve from the cit-AgNP surface and complex readily with the thiol group of MT, which is also
11 highly induced by cit-AgNP (Figure 4B). It should be noted that in L-15/ex medium, cit-AgNP
12 suspension shows ~7% dissolution (Figure 2) thus fitting the 5-7% of Ag-cysteine complexes.
13 Previous studies, where mammalian cells have been exposed to AgNP for 24 hours showed
14 38%³³, 30-80%¹⁶, 43%³⁴, 61%⁴², and 51-73%⁴⁰ of total accumulated silver as Ag⁰-NP, which
15 suggests that in mammalian cells a higher percentage of silver is dissolved intracellularly from
16 the nanoparticle surface compared to the fish intestinal cells. The second most important silver
17 species in common with other mammalian studies and our fish cells study is Ag-S- (most likely
18 Ag complexed with the thiol group in glutathione or metallothionein) which was detected at
19 61%³³, 20-50%¹⁶, 33%³⁴, 39%⁴², and 21-46%⁴⁰. In addition, Ag-O- was detected at 26%³⁴, 10-
20 20%¹⁶ and 2%⁴⁰ and AgCl at 10-30%¹⁶ and 3-4%⁴⁰. A couple of considerations should be made
21 when comparing exposures in mammalian cells and our study which used fish cells: i)
22 mammalian cells are cultured at 37°C whereas fish cells are cultured at 19°C which results in a
23 higher cell metabolism⁴³; ii) the mammalian studies have used concentrations 10 times higher
24 than our study which might have resulted in a higher intercellular stress response. As
25 mentioned earlier, the doses of AgNO₃ and cit-AgNP were not toxic, suggesting that at this
26 concentration, MT is able to scavenge most dissolved silver in the cell. Remarkably, in cells
27 exposed to AgNO₃ and cit-AgNP for 72 hours MT mRNA levels drop significantly in comparison
28 to levels shown in cells exposed for 24 hours while silver concentration increases. This can be
29
30
31
32
33
34
35
36
37
38
39
40
41
42
43
44
45
46
47
48
49
50
51
52
53
54
55
56
57
58
59
60

1
2
3 explained by the fact that almost all dissolved Ag is complexed to cysteine which detoxifies
4 silver and inhibits the induction of MT mRNA levels, an effect previously shown in RTgutGC
5 cells exposed to cit-AgNP¹¹.
6
7
8
9

10 11 **Conclusions**

12
13
14 This study shows how analysis of extracellular and intracellular metal speciation can clarify
15 the intracellular chemical fate of metals and metal nanoparticles. Moreover, this approach brings
16 a new insight to our understanding of Ag and cit-AgNP uptake and bio-reactivity in fish intestinal
17 cells. One major aspect of this study is that while most aquatic toxicology literature indicates
18 that fish can readily take up Ag⁺ but not AgCl complexes, our data show that the intestinal cell
19 RTgutGC can take up (or adsorb) silver as AgCl complexes, which are subsequently
20 bioavailable and bio-reactive. Although the intestine is not a major target of waterborne silver in
21 fresh water (freshwater fish do not drink), these results could explain the enhanced toxicity of
22 silver at high salinities (i.e. seawater)^{8,12}, where fish drink to osmoregulate⁴⁴.
23
24
25
26
27
28
29
30
31
32

33 Moreover, it was shown in *in vitro* (²⁵ and Figure 3C), *ex vivo*³⁷ and *in vivo*⁴⁵ studies that the
34 intestinal epithelium accumulates similar concentrations of silver when exposed to equimolar
35 amounts of AgNO₃ or AgNP. However, at least in *in vitro* studies cit-AgNP is about 10-15 times
36 less toxic than AgNO₃^{11,22,46}. In this study, we demonstrate that at equimolar amounts of
37 intracellular silver concentrations AgNO₃ is more toxic than cit-AgNP, at least after acute
38 exposures (i.e., 24 hours). The intracellular silver speciation therefore supports the hypothesis
39 that dissolved silver species are more toxic than zero-valent silver nanoparticles. Overall, our
40 data supports previous *in vivo*⁴⁵ and *in vitro*²⁵ studies where silver nanoparticles present a
41 similar but attenuated toxic response to ionic silver (AgNO₃). Thus, at least in acute exposures,
42 existing risk assessment for dissolved silver species would also be protective for nano-silver.
43
44
45
46
47
48
49
50
51
52
53
54 However, under chronic exposure scenarios an increase in silver nanoparticle toxicity cannot be
55 excluded due to a potential increase in intracellular silver dissolution.
56
57
58
59
60

Conflicts of interest

There are no conflicts to declare

Acknowledgements

This research was supported by the U.S. National Science Foundation (NSF) Biological and Environmental Interactions of Nanoscale Materials program through award nos. CBET-1706093 (M.M.) and CBET-1704362 (J.G.C.). The XAS measurements were performed at the DuPont-Northwestern-Dow Collaborative Access Team (DND-CAT) located at Sector 5 of the Advanced Photon Source (APS). DND-CAT is supported by Northwestern University, E.I. DuPont de Nemours & Co., and The Dow Chemical Company. This research used resources of the Advanced Photon Source, a U.S. Department of Energy (DOE) Office of Science User Facility operated for the DOE Office of Science by Argonne National Laboratory under Contract No. DE-AC02-06CH11357. The authors wish to thank Professor Kristin Schirmer (eawag, CH) for providing the cell line RTgutGC used in this study.

References

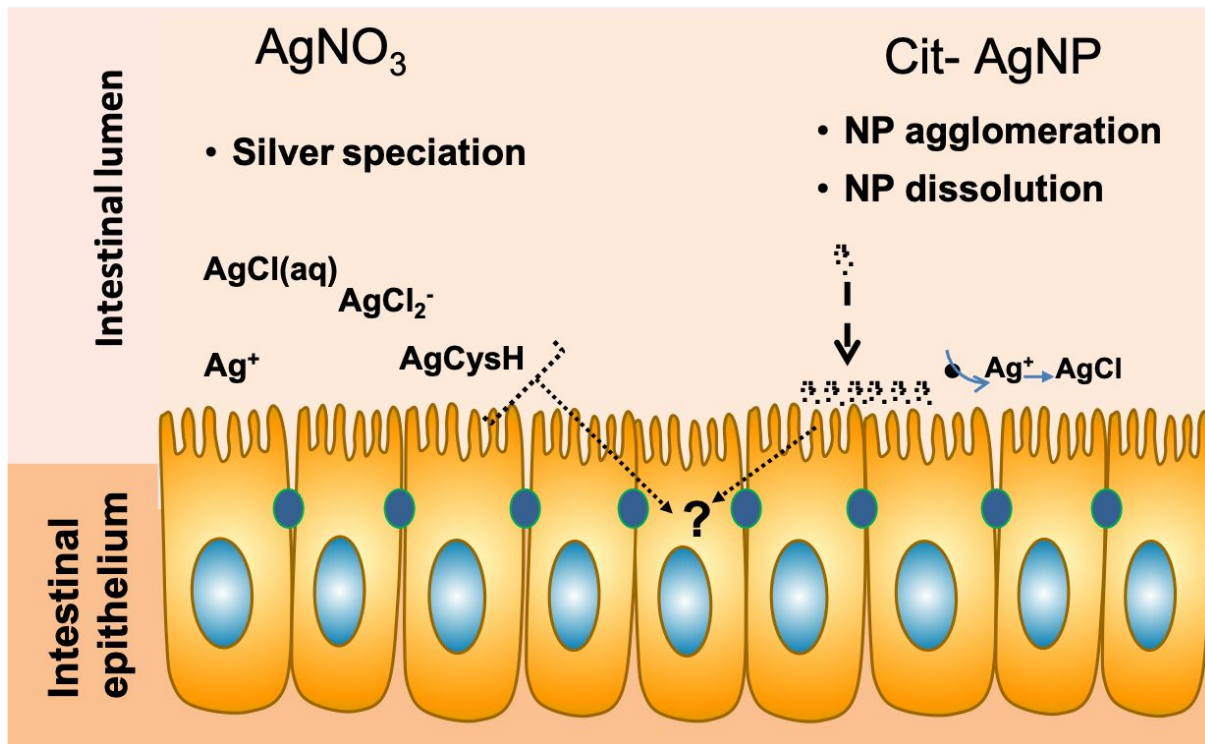
- 1 EU, Commission Recommendation of 18 October 2011 On The Definition of Nanomaterial (2011/696/EU), Off. J. Eur. Union, 2011, 275, 38–40.
- 2 R. Behra, L. Sigg, M. J. D. Clift, F. Herzog, M. Minghetti, B. Johnston, A. Petri-Fink, B. Rothen-Rutishauser and B. Rothen-Rutishauser, Bioavailability of silver nanoparticles and ions : from a chemical and biochemical perspective, J. R. Soc. Interface, 2013, 10, 20130396.
- 3 J. R. Morones-Ramirez, J. A. Winkler, C. S. Spina and J. J. Collins, Silver enhances antibiotic activity against gram-negative bacteria, Sci. Transl. Med. , 2013, 5, 190ra81-190ra81.
- 4 E. K. Hill and J. Li, Current and future prospects for nanotechnology in animal production, J. Anim. Sci. Biotechnol., 2017, 8, 1–13.
- 5 P. Swain, S. K. Nayak, A. Sasmal, T. Behera, S. K. Barik, S. K. Swain, S. S. Mishra, A. K. Sen, J. K. Das and P. Jayasankar, Antimicrobial activity of metal based nanoparticles against microbes associated with diseases in aquaculture, World J. Microbiol. Biotechnol., 2014, 30, 2491–2502.
- 6 P. R. Paquin, J. W. Gorsuch, S. Apte, G. E. Batley, K. C. Bowles, P. G. C. Campbell, C. G. Delos, D. M. Di Toro, R. L. Dwyer, F. Galvez, R. W. Gensemer, G. G. Goss, C.

- 1
2
3 Hogstrand, C. R. Janssen, J. C. McGeer, R. B. Naddy, R. C. Playle, R. C. Santore, U.
4 Schneider, W. A. Stubblefield, C. M. Wood and K. B. Wu, The biotic ligand model: a
5 historical overview, *Comp. Biochem. Physiol. Part C Toxicol. Pharmacol.*, 2002, 133, 3–
6 35.
- 7 J. Genz, A. J. Esbaugh and M. Grosell, Intestinal transport following transfer to increased
8 salinity in an anadromous fish (*Oncorhynchus mykiss*), *Comp. Biochem. Physiol. A. Mol.*
9 *Integr. Physiol.*, 2011, 159, 150–8.
- 10 E. A. Ferguson and C. Hogstrand, Acute silver toxicity to seawater-acclimated rainbow
11 trout: Influence of salinity on toxicity and silver speciation, *Environ. Toxicol. Chem.*, 1998,
12 17, 589–593.
- 13 C. M. Zhao, P. G. C. Campbell and K. J. Wilkinson, When are metal complexes
14 bioavailable?, *Environ. Chem.*, 2016, 13, 425–433.
- 15 N. R. Bury and C. Hogstrand, Influence of chloride and metals on silver bioavailability to
16 Atlantic salmon (*Salmo salar*) and Rainbow trout (*Oncorhynchus mykiss*) yolk-sac fry,
17 *Environ. Sci. Technol.*, 2002, 36, 2884–8.
- 18 M. Minghetti and K. Schirmer, Effect of media composition on bioavailability and toxicity
19 of silver and silver nanoparticles in fish intestinal cells (RTgutGC), *Nanotoxicology*, 2016,
20 10, 1526–1534.
- 21 C. W. Matson, A. J. Bone, M. M. M. M. Auffan, T. T. Lindberg, M. C. Arnold, H. Hsu-Kim,
22 M. R. Wiesner and R. T. Di Giulio, Silver toxicity across salinity gradients: the role of
23 dissolved silver chloride species (AgCl_x) in Atlantic killifish (*Fundulus heteroclitus*) and
24 medaka (*Oryzias latipes*) early life-stage toxicity, *Ecotoxicology*, 2016, 25, 1105–1118.
- 25 C. M. Wood, R. C. Playle and C. Hogstrand, Physiology and modeling of mechanisms of
26 silver uptake and toxicity in fish, *Environ. Toxicol. Chem.*, 1999, 18, 71–83.
- 27 J. Bertinato, L. Cheung, R. Hoque and L. J. Plouffe, Ctr1 transports silver into mammalian
28 cells, *J. Trace Elem. Med. Biol.*, 2010, 24, 178–184.
- 29 M. I. Setyawati, X. Yuan, J. Xie and D. T. Leong, The influence of lysosomal stability of
30 silver nanomaterials on their toxicity to human cells, *Biomaterials*, 2014, 35, 6707–15.
- 31 I.-L. Hsiao, Y.-K. Hsieh, C.-F. Wang, I.-C. Chen and Y.-J. Huang, Trojan-horse
32 Mechanism in the Cellular Uptake of Silver Nanoparticles Verified by Direct Intra- and
33 Extracellular Silver Speciation Analysis, *Environmental Sci. Technol.*, 2015, 49, 3813–21.
- 34 J. H. Kaplan and S. Lutsenko, Copper transport in mammalian cells: Special care for a
35 metal with special needs, *J. Biol. Chem.*, 2009, 284, R109.
- 36 C. Levard, E. M. Hotze, B. P. Colman, A. L. Dale, L. Truong, X. Y. Yang, A. J. Bone, G.
37 E. Brown, R. L. Tanguay, R. T. Di Giulio, E. S. Bernhardt, J. N. Meyer, M. R. Wiesner and
38 G. V. Lowry, Sulfidation of silver nanoparticles: Natural antidote to their toxicity, *Environ.*
39 *Sci. Technol.*, 2013, 47, 13440–13448.
- 40 M. Auffan, C. W. Matson, J. Rose, M. Arnold, O. Proux, B. Fayard, W. Liu, P. Chaurand,
41 M. R. Wiesner, J.-Y. Bottero and R. T. Di Giulio, Salinity-dependent silver nanoparticle
42 uptake and transformation by Atlantic killifish (*Fundulus heteroclitus*) embryos,
43 *Nanotoxicology*, 2014, 8, 167–176.
- 44 K. J. Groh, T. Dalkvist, F. Piccapietra, R. Behra, M. J.-F. Suter and K. Schirmer, Critical
45 influence of chloride ions on silver ion-mediated acute toxicity of silver nanoparticles to
46 zebrafish embryos. *Nanotoxicology*, 2015, (1):81-91
- 47 M. Minghetti, C. Drieschner, N. Bramaz, H. Schug and K. Schirmer, A fish intestinal
48 epithelial barrier model established from the rainbow trout (*Oncorhynchus mykiss*) cell
49 line, RTgutGC, *Cell Biol. Toxicol.*, 2017, 33, 539–555.
- 50 Y. Yue, R. Behra, L. Sigg, P. Fernández Freire, S. Pillai and K. Schirmer, Toxicity of silver
51 nanoparticles to a fish gill cell line: Role of medium composition, *Nanotoxicology*, 2015, 9,
52 54–63.
- 53 J. A. Rees, G. J. P. Deblonde, D. D. An, C. Ansoborlo, S. S. Gauny and R. J. Abergel,
54
55
56
57
58
59
60

- 1
2
3 Evaluating the potential of chelation therapy to prevent and treat gadolinium deposition
4 from MRI contrast agents, *Sci. Rep.*, 2018, 8, 2–10.
- 5 24 R. Ortega, Direct speciation analysis of inorganic elements in single cells using X-ray
6 absorption spectroscopy, *J. Anal. At. Spectrom.*, 2011, 26, 23–29.
- 7 25 M. Minghetti and K. Schirmer, Interference of silver nanoparticles with essential metal
8 homeostasis in a novel enterohepatic fish in vitro system, *Environ. Sci. Nano*, 2019, 6,
9 1777.
- 10 26 S. Roudeau, A. Carmona, L. Perrin and R. Ortega, Correlative organelle fluorescence
11 microscopy and synchrotron X-ray chemical element imaging in single cells, *Anal.*
12 *Bioanal. Chem.*, 2014, 406, 6979–6991.
- 13 27 S. Beauchemin, D. Hesterberg, J. Nadeau and J. C. McGeer, Speciation of hepatic Zn in
14 trout exposed to elevated waterborne Zn using X-ray absorption spectroscopy, *Environ.*
15 *Sci. Technol.*, 2004, 38, 1288–1295.
- 16 28 R. Sekine, G. Brunetti, E. Donner, M. Khaksar, K. Vasilev, A. K. Jämting, K. G. Scheckel,
17 P. Kappen, H. Zhang and E. Lombi, Speciation and lability of Ag-, AgCl-, and Ag₂S-
18 nanoparticles in soil determined by X-ray absorption spectroscopy and diffusive gradients
19 in thin films, *Environ. Sci. Technol.*, 2015, 49, 897–905.
- 20 29 S. D. Kelly, D. Hestberg and B. Ravel, in *Methods of Soil Analysis, Part 5 - Mineralogical*
21 *Methods*, Soil Science Society of America, Madison, WI, 2008, pp. 367–463.
- 22 30 B. Ravel and M. Newville, ATHENA, ARTEMIS, HEPHAESTUS: data analysis for X-ray
23 absorption spectroscopy using IFEFFIT, *J. Synchrotron Radiat.*, 2005, 12, 537–541.
- 24 31 M. Newville, IFEFFIT: interactive XAFS analysis and FEFF fitting, *J. Synchrotron Radiat.*,
25 2001, 8, 322–324.
- 26 32 A. Manceau, M. A. Marcus and N. Tamura, Quantitative Speciation of Heavy Metals in
27 Soils and Sediments by Synchrotron X-ray Techniques, *Rev. Mineral. Geochemistry*,
28 2002, 49, 341–428.
- 29 33 X. Jiang, T. Miclăuș, L. Wang, R. Foldbjerg, D. S. Sutherland, H. Autrup, C. Chen and C.
30 Beer, Fast intracellular dissolution and persistent cellular uptake of silver nanoparticles in
31 CHO-K1 cells: implication for cytotoxicity, *Nanotoxicology*, 2015, 9, 181–189.
- 32 34 L. Wang, T. Zhang, P. Li, W. Huang, J. Tang, P. Wang, J. Liu, Q. Yuan, R. Bai, B. Li, K.
33 Zhang, Y. Zhao and C. Chen, Use of Synchrotron Radiation-Analytical Techniques To
34 Reveal Chemical Origin of Silver-Nanoparticle Cytotoxicity, *ACS Nano*, 2015, 9, 6532–
35 6547.
- 36 35 Y.-H. Lee, F.-Y. Cheng, H.-W. Chiu, J.-C. Tsai, C.-Y. Fang, C.-W. Chen and Y.-J. Wang,
37 Cytotoxicity, oxidative stress, apoptosis and the autophagic effects of silver nanoparticles
38 in mouse embryonic fibroblasts, *Biomaterials*, 2014, 35, 4706–15.
- 39 36 E. Navarro, F. Piccapietra, B. Wagner, B. Wagner, F. Marconi, F. Marconi, R. Kaegi, R.
40 Kaegi, N. Odzak and N. Odzak, Toxicity of Silver Nanoparticles to *Chlamydomonas*
41 *reinhardtii*, *Environ. Sci. Technol.*, 2008, 42, 8959–8964.
- 42 37 N. J. Clark, D. Boyle and R. D. Handy, An assessment of the dietary bioavailability of
43 silver nanomaterials in rainbow trout using an ex vivo gut sac technique, *Environ. Sci.*
44 *Nano*, 2019, 6, 646–660.
- 45 38 M. Minghetti, M. J. J. Leaver, E. Carpenè and S. G. G. George, Copper transporter 1,
46 metallothionein and glutathione reductase genes are differentially expressed in tissues of
47 sea bream (*Sparus aurata*) after exposure to dietary or waterborne copper, *Comp.*
48 *Biochem. Physiol. Part C Toxicol. Pharmacol.*, 2008, 147, 450–459.
- 49 39 Y. Nose, B.-E. E. Kim and D. J. Thiele, Ctr1 drives intestinal copper absorption and is
50 essential for growth, iron metabolism, and neonatal cardiac function, *Cell Metab.*, 2006,
51 4, 235–244.
- 52 40 G. Veronesi, A. Deniaud, T. Gallon, P.-H. Jouneau, J. Villanova, P. Delangle, M. Carrière,
53 I. Kieffer, P. Charbonnier, E. Mintz and I. Michaud-Soret, Visualization, quantification and
54
55
56
57
58
59
60

coordination of Ag⁺ ions released from silver nanoparticles in hepatocytes, *Nanoscale*, 2016, 8, 17012–17021.

- 41 A. B. G. Lansdown, A Pharmacological and Toxicological Profile of Silver as an
Antimicrobial Agent in Medical Devices, *Adv. Pharmacol. Sci.*, 2010, 2010, 1–16.
- 42 G. Veronesi, C. Aude-Garcia, I. Kieffer, T. Gallon, P. Delangle, N. Herlin-Boime, T.
Rabilloud and M. Carrière, Exposure-dependent Ag⁺ release from silver nanoparticles
and its complexation in AgS₂ sites in primary murine macrophages, *Nanoscale*, 2015, 7,
7323–7330.
- 43 P. Ducommun, P. A. Ruffieux, A. Kadouri, U. Von Stockar and I. W. Marison, Monitoring
of temperature effects on animal cell metabolism in a packed bed process, *Biotechnol.
Bioeng.*, 2002, 77, 838–842.
- 44 D. H. Evans, Teleost fish osmoregulation: what have we learned since August Krogh,
Homer Smith, and Ancel Keys, *Am. J. Physiol. Integr. Comp. Physiol.*, 2008, 295, R704–
R713.
- 45 N. J. Clark, D. Boyle, B. P. Eynon and R. D. Handy, Dietary exposure to silver nitrate
compared to two forms of silver nanoparticles in rainbow trout: bioaccumulation potential
with minimal physiological effects, *Environ. Sci.: Nano*, 2019, 6, 1393–1405
- 46 M. Connolly, M.-L. Fernandez-Cruz, A. Quesada-Garcia, L. Alte, H. Segner and J. M.
Navas, Comparative Cytotoxicity Study of Silver Nanoparticles (AgNPs) in a Variety of
Rainbow Trout Cell Lines (RTL-W1, RTH-149, RTG-2) and Primary Hepatocytes, *Int. J.
Environ. Res. Public Health*, 2015, 12, 5386–405.



1
2
3 **Figure 1:** Conceptual representation of the measurable chemical transformations of dissolved
4 silver and cit-AgNP in the intestinal lumen. Such transformations influence intracellular metal
5 uptake, speciation and bio-reactivity. Analysis of dissolved silver and cit-AgNP transformations
6 in extracellular medium include metal speciation (Visual MINTEQ), NP agglomeration (Dynamic
7 Light Scattering) and NP dissolution (ultracentrifugation and ultrafiltration)^{11,22}. Intracellular
8 transformations can be determined by X-ray absorption spectroscopy.
9
10
11
12
13
14
15
16
17
18
19
20
21
22
23
24
25
26
27
28
29
30
31
32
33
34
35
36
37
38
39
40
41
42
43
44
45
46
47
48
49
50
51
52
53
54
55
56
57
58
59
60

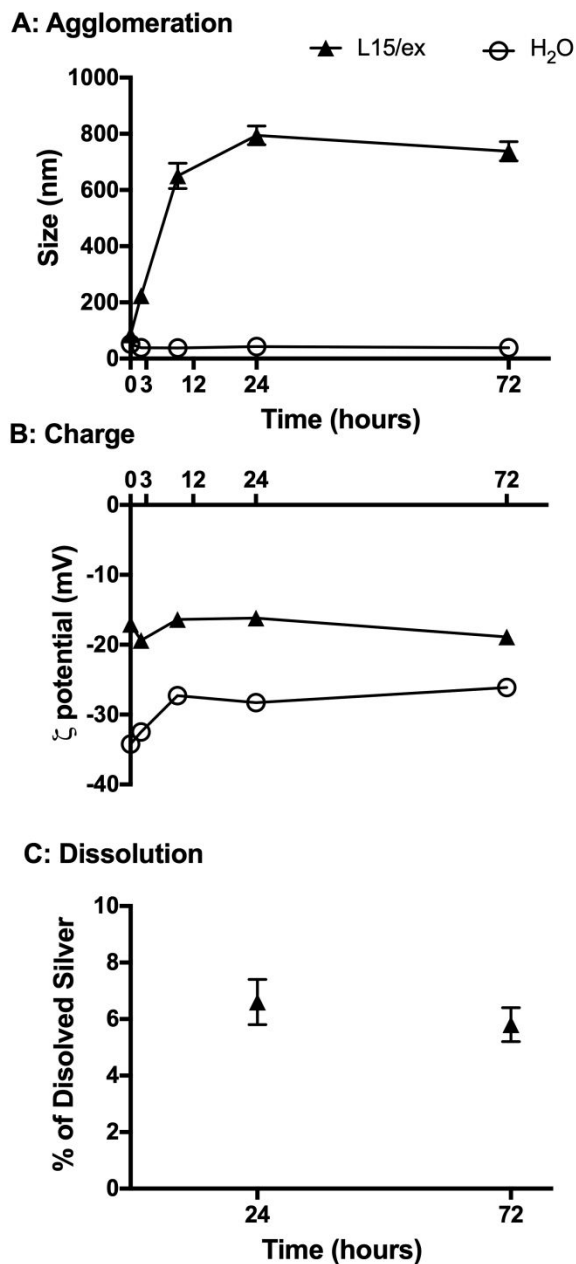


Figure 2: Cit-AgNP characterization. Size and ζ -potential of 10 μ M cit-AgNP in L15-ex and water over 72 hours is reported in panel A and B, respectively. Dissolution in L-15/ex is reported in panel C. The cit-AgNP size (Z-average) and ζ potential of cit-AgNP suspensions were measured in triplicate by DLS and dissolution by ultracentrifugation. Values are mean \pm SD, $n=3$.

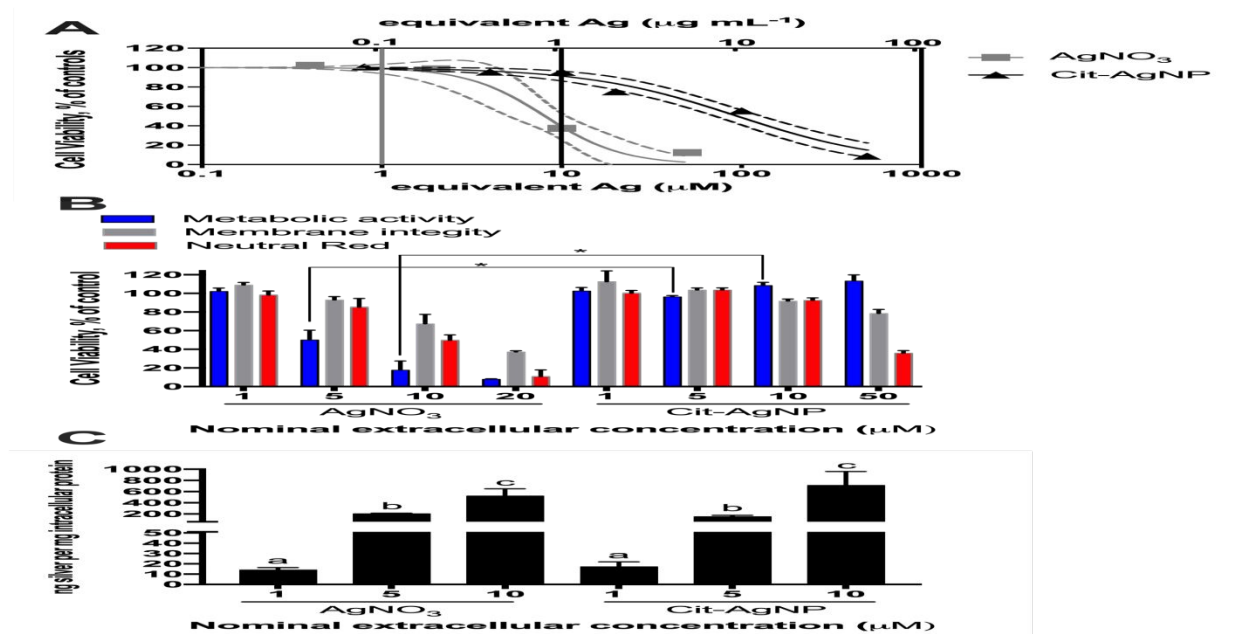
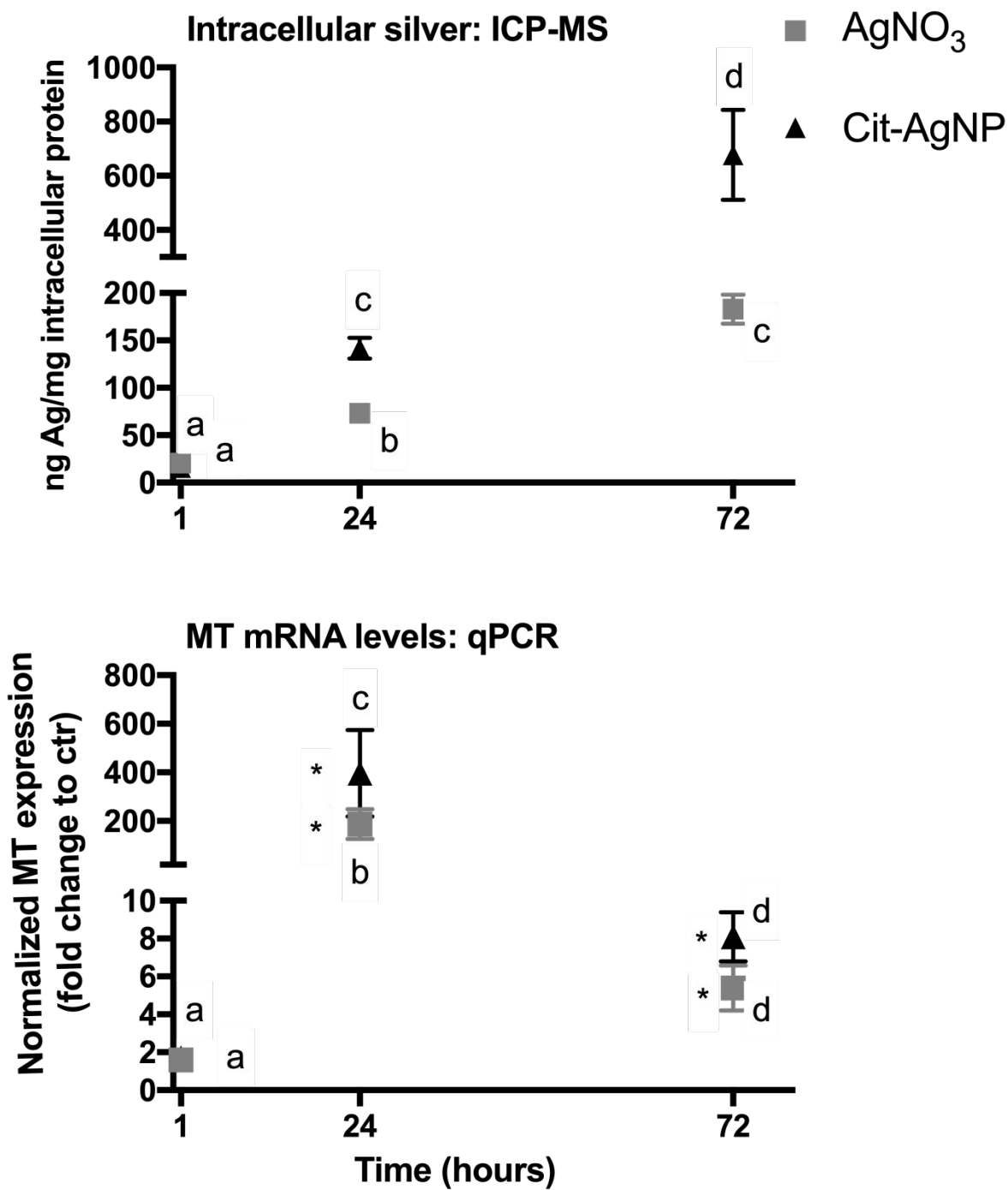
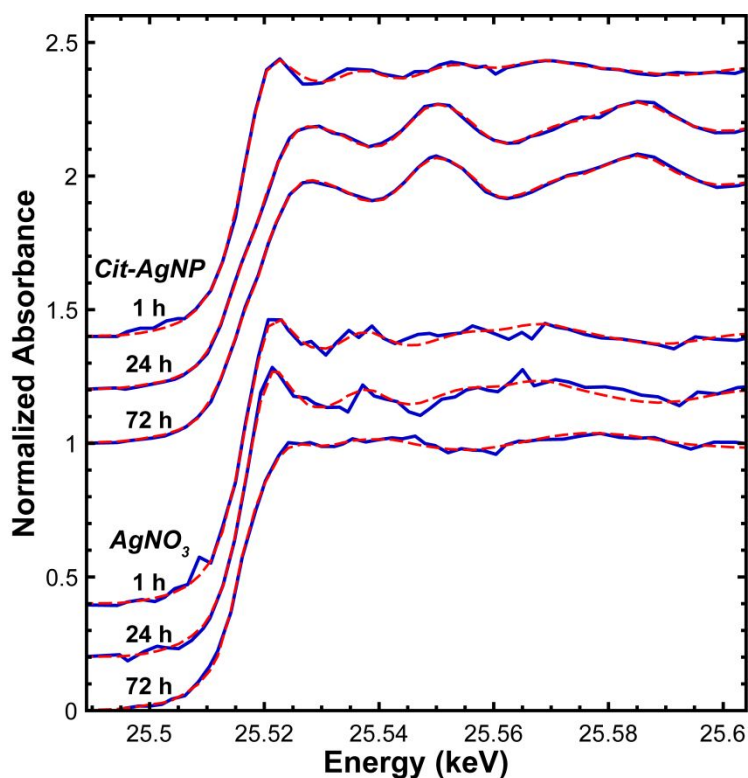


Figure 3: Toxicity of AgNO₃ and cit-AgNP as function of total silver in the exposure medium (L-15/ex). The endpoints measured, cell metabolic activity, cell membrane integrity and lysosome integrity, were taken after 24 hours of exposure. A, AgNO₃ and cit-AgNP dose-response curve using the cell membrane integrity endpoint (CFDA-AM). Values shown are averages and confidence intervals (dashed lines) of three independent experiments (n=3). Exposure concentrations of AgNO₃ (1 μM or 0.108 μg/mL) and cit-AgNP (10 μM or 1.08 μg/mL) are indicated by a vertical line. A double scale of equivalent silver is shown for comparison. B, multiple endpoint viability assay in RTgutGC cells exposed for 24 hours, values shown are a means ± SD (n=3). Differences in metabolic activity in cells exposed to equimolar concentrations of AgNO₃ and cit-AgNP (i.e., 1, 5 and 10 μM) are indicated by an asterisk (1-way, p<0.05, 1-way ANOVA, Tukey's test). C, silver concentration determined by ICP-MS in RTgutGC cells exposed for 24 hours. Cellular-associated silver was normalized to protein content to consider possible variation in cell numbers. Values are means ± SD, n=4. Bars bearing different lettering are significantly different (p < 0.05, 1-way ANOVA, Tukey's test).



51 **Figure 4:** Intracellular silver uptake and bio-reactivity in RTgutGC exposed to non-toxic doses of
52 AgNO₃ (1 μ M or 0.108 μ g/mL) and cit-AgNP (10 μ M or 1.08 μ g/mL) over 72 hours. A: Total
53 silver determination by ICP-MS. Metal concentration in cell lysates is reported as ng silver per
54
55
56
57
58
59
60

1
2
3 mg of protein determined from the same samples to take into account differences in cell
4
5 numbers. Values represent mean \pm SD, $n=3$. Symbols bearing different lettering are statistically
6
7 different ($p<0.05$, 2-way ANOVA, Tukey's test). B: Normalized mRNA levels of Metallothionein
8
9 (MT). Values are expressed as ratio of the expression in those cells exposed to control media
10
11 (see Figure S3). Values represent mean normalized fold change \pm SD, $n=3$. Symbols bearing
12
13 different lettering are statistically different ($p<0.05$, 2-way ANOVA, Tukey's test). Statistical
14
15 difference from respective control, i.e., untreated cells at each time point is indicated by an
16
17 asterisk (t-test, $p<0.05$).
18
19
20
21



22
23
24
25
26
27
28
29
30
31
32
33
34
35
36
37
38
39
40
41
42
43
44
45
46
47 **Figure 5:** Ag K-edge XANES spectra of pelleted RTgutGC cells exposed to either silver
48 nanoparticles (Cit-AgNP) or silver nitrate solution (AgNO_3). The data (solid blue) were fitted
49 (dashed red) as a linear combination of the spectra of Ag chloride, Ag cysteine, or Ag
50 nanoparticles (see Figure 6). Fitting procedures, statistical assessment of spectral variability
51
52
53
54
55
56
57
58
59
60

and appropriate fitting standards, and detailed fitting results are reported in the Supplementary Information.

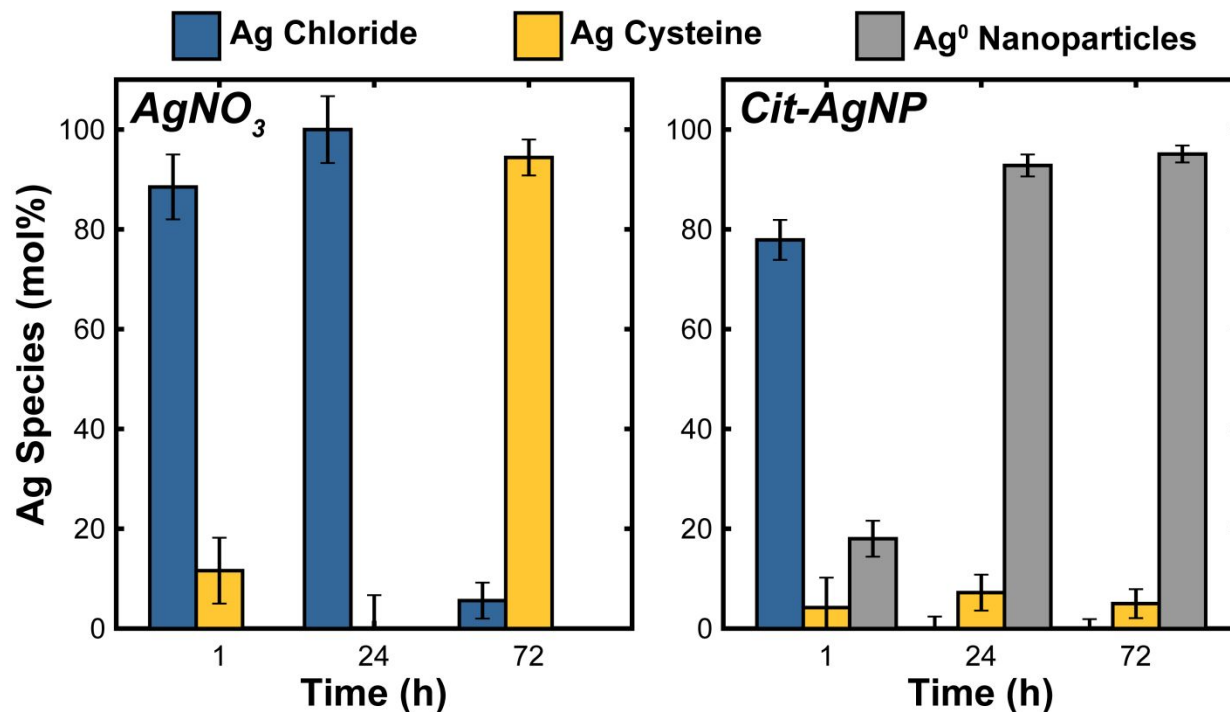


Figure 6: Intracellular silver speciation determined by linear combination fitting of the XANES spectra reported in Figure 5. Values are the molar percentages of the total Ag species in the samples, with the error bar indicating the uncertainties derived from the linear-combination fitting procedure, reported at the 1 σ level (68% confidence interval).

